Journal of Reproduction and Development, Vol. 62, No 4, 2016

—Original Article—

Involvement of Transient Receptor Potential Vanilloid (TRPV) 4 in mouse sperm thermotaxis

Koh-ichi HAMANO[1)], Tae KAWANISHI[1)], Atsuko MIZUNO[2)], Makoto SUZUKI[2)] and Yuji TAKAGI[1)]

[1)] *Faculty of Agriculture, Shinshu University, Nagano 399-4598, Japan*
[2)] *Molecular Pharmacology, Jichi Medical School, Tochigi 329-0498, Japan*

Abstract. Transient Receptor Potential Vanilloid (TRPV) 4 is one of the temperature-sensitive ion channels involved in temperature receptors, and it is known to be activated from 35 to 40ºC. Here we analyzed sperm motility function of *Trpv4* knockout (KO) mouse in temperature-gradient conditions to elucidate the thermotaxis of mouse sperm and the involvement of TRPV4 in thermotaxis. The sperm were introduced at the vertical column end of a T-shaped chamber filled with medium in a plastic dish, and we measured the number of sperm that arrived at both ends of the wide column where we had established a temperature gradient of approx. 2ºC, and we evaluated the sperm's thermotaxis. Large numbers of wild-type (WT) mouse sperm migrated into the high level of the temperature gradient that was set in the wide column, and thermotaxis was confirmed. The ratio of migrated sperm at the high temperature level of the T-shaped chamber was decreased in the KO sperm and Ruthenium red (a TRPV antagonist) treated sperm compared with the WT sperm. The thermotaxis of the mouse sperm was confirmed, and the involvement of TRPV4 in this thermotaxis was suggested.

Key words: Mouse, Sperm, Thermotaxis, Transient Receptor Potential Vanilloid (TRPV) 4

(**J. Reprod. Dev. 62:** 415–422, 2016)

Mammalian sperm ejaculated into a female reproductive tract migrate to the fertilization site due to the effects of multiple factors, and then they penetrate an oocyte and fertilize it. Chemotaxis has also been described in bacteria [1] and marine animals [2], and in mammals the chemotaxis of sperm that migrated toward chemical attractants in the cumulus cells and follicular fluid was confirmed [3]. In bacteria, the chemotactic receptors are thermo-sensors that are involved in thermotaxis [1, 4]. David *et al*. [5] and Hunter and Nichol [6] reported that in the rabbit and the boar, the differences in temperature between the isthmus of the oviduct (i.e., the sperm storage site) and the ampulla of the oviduct (the fertilization site) at ovulation were approx. 2ºC and 0.7ºC, respectively.

These findings raise the possibility that the difference in temperature in a female genital tract induces sperm to move to the fertilization site. In an *in vitro* study, Bahat *et al*. [7] reproduced a 2ºC difference in temperature in the rabbit reproductive tract, and they reported that positive thermotaxis was demonstrated because capacitated rabbit sperm migrated to the high-temperature area. They carried out a similar experiment in human sperm and confirmed positive thermotaxis [8]. Bahat *et al*. [7, 9] speculated that thermotaxis and chemotaxis act complementarily in the rabbit oviduct.

Because a sperm chemoattractant spreads by oviductal peristalsis, it is difficult for sperm to migrate to the fertilization site only via chemotaxis. Thermotaxis is effective for the migration of rabbit sperm from the isthmus to the ampulla of the oviduct, in which there is a temperature difference at ovulation. Sperm are induced to travel to the oocyte primarily by chemotaxis, but they do not appear to be regulated by thermotaxis. Rabbit sperm were reported to have a very sensitive thermo-sensing ability (0.16ºC/cm) [9, 10].

Capacitated rabbit or human sperm were reported to migrate toward a warmer fertilization site from a low-temperature site by thermotaxis and then swim to cumulus oocyte complex by chemotaxis and subsequently approach the egg [9, 11, 12]. Thermotaxis is thus thought to be an important physiological function of mammalian sperm in a female genital tract. The regulation and the underlying mechanisms of thermotaxis by mammalian sperm are still largely unknown.

A temperature-sensitive mechanism in eukaryotic cells is known to depend on the involvement of the temperature-sensitive ion channel of the Transient Receptor Potential (TRP) family. This family includes four heat-gated ion channels (TRPV1, 2, 3, and 4) [13] and two low-temperature thermo-sensors (TRPM8 and TRPA1) [14]. The temperature-sensitive TRP channels are divided into three groups by the temperature levels that they sense. TRPV3 and TRPV4 sense thermal stimuli at 30–40ºC and are localized mostly in the skin epidermal cells [15–17]. *Trpv3* or *Trpv4* gene-deficient mice were shown to respond an optimal temperature that differed from that by wild-type (WT) mice in behavior studies [18, 19], revealing that these genes are important to the temperature perception at the living body level [20].

TRPV1 was detected in rat testes [21], and TRPV4 was detected in the boar sperm head [22]. Some members of the TRPC subfamilies

Received: July 24, 2015
Accepted: April 28, 2016
Published online in J-STAGE: May 16, 2016

Correspondence: K Hamano (e-mail: khamano@shinshu-u.ac.jp)

were identified in the head or tail of mouse or human sperm [23, 24]. TRPM8 was identified in both the head and tail of human sperm, and it was suggested to be involved in an increase in the intracellular Ca^{2+} in response to a temperature decrease or ligand binding [25]. However, there is no evidence that these TRPC Ca^{2+} channels function as thermo-sensors. Bahat *et al*. demonstrated that the IP3R Ca^{2+} channel is involved in human sperm thermotaxis, and that the response of sperm to thermotaxis was regulated by phospholipase C (PLC) and required intracellular Ca^{2+}. It thus appears that the thermo-sensors of thermotaxis are not any of the known chemotactic receptors.

In the present study, we examined sperm migration and motility using a *Trpv4* genetic defect mouse to examine the thermotaxis of mouse sperm and the involvement of TRPV4 in mouse sperm thermotaxis.

Materials and Methods

Media and chemicals

We used TYH medium (Toyoda, Yokoyama and Hoshi [26]) for mouse *in vitro* fertilization, and it contained bovine serum albumin (BSA; Wako, Tokyo, Japan). Sperm pre-incubation was conducted in a micro-drop of TYH in the 37ºC, 5% CO_2/95% air of a CO_2 incubator. Ruthenium red (a TRPV antagonist) was purchased from Sigma-Aldrich (St Louis, MO, USA), and all other reagent-grade chemicals were purchased from Wako Pure Chemicals (Osaka, Japan) unless otherwise indicated.

Animals

Wild-type (WT) C57BL/6J male mice were purchased from Japan SLC (Shizuoka, Japan). *Trpv4* gene-deficient (−/−) knockout (KO) male mice were prepared by backcrossing four generations onto a C57BL/6J background according to the method of Mizuno and others [18]. Sexually mature male WT and KO mice were maintained in a light-controlled room (12 h light/12 h dark). All experiments were conducted according to the animal experiment guidelines of Shinshu University. This study was approved by the Committee on the Ethical Treatment of Experimental Animals at Shinshu University (Approval ID: 1929).

Gene expression analysis of testicular cells

The tunica albuginea of the testes of mature WT and KO mice was exfoliated after being washed with phosphate-buffered saline (PBS). The total RNA of the testicular cells was extracted using TRIzol reagent (Invitrogen, Carlsbad, CA, USA) according to the manufacturer's instructions. We made cDNA from the total RNA of the testicular cells by a reaction with reverse transcription using Rever Tra Ace (Toyobo, Tokyo, Japan) and an oligo-dT primer, RNase inhibitor (Toyobo). The polymerase chain reaction (PCR) used two specific primers (Table 1). The PCR reaction consisted of 40 cycles (95ºC for 30 sec, 58ºC for 1 min and 72ºC for 1 min) after denaturation in 94ºC for 5 min, and the definitive extension was carried out at 72ºC for 5 min. We confirmed the identity of the sequence by checking it against the inspection database NCBI BLAST program.

Spermatogenesis and sperm morphology analysis

Spermatogenesis analysis: The testes of WT mouse and *Trpv4* KO mouse were removed and immersion-fixed in Bouin's solution for 24 h. Following fixation, testes were dehydrated in ethanol and embedded in paraffin. The 5 µm-thick sections were deparaffinized, dehydrated and treated with periodic acid-Schiff (PAS) and hematoxylin. The PAS stained tissue samples were examined normality from morphology of seminiferous tubule and germ cell. Sperm morphology analysis: Sperm recovered from cauda epididymis were immersion-fixed in 4% paraformaldehyde (pH = 7.4) for 10 min. The sedimented sperm after centrifugation (1500 rpm, 5 min) were washed twice with 100 mM ammonium acetate and dropped by 200 µl to the coat slide glass equipped with flexiPERM (Greiner Bio-one, Tokyo, Japan) and adhered to slide glass by centrifugation (1500 rpm, 10 min). The air dried sperm specimen were stained with Coomassie staining solution and evaluated the sperm morphology and acrosomal normality.

Immunocytochemical analysis

Sperm recovered from the cauda epididymis was dropped in 200 µl amounts onto slide glasses equipped with flexiPERM (Greiner Bio-one, Tokyo, Japan) and adhered by centrifugation (1500 rpm, 10 min). The sperm specimens were washed with phosphate-buffered saline (PBS) after fixation with 4% paraformaldehyde for 10 min at 4ºC and washed again with PBS after 30 min treatment by 0.5% TritonX-100. The specimen were treated with blocking buffer (Roshe, Tokyo, Japan) for 30 min and reacted with rabbit anti-mouse TRPV4 antibody (1:100) (Alomone Labs, Jerusalem, Israel) overnight at room temperature. After being washed with PBS, the specimen were reacted with Cy3-labeled goat anti-rabbit IgG antibody (1:50) (Chemicon, NY, USA) for 30 min at room temperature and washed with PBS. The negative control was reacted with normal rabbit immunoglobulin overnight at room temperature, and then subjected to the following processing. We examined the specimens with a microscope (BX40, Olympus, Tokyo, Japan) equipped with fluorescence device (BX-FLA, Olympus).

Evaluation of sperm motility and thermotaxis

The sperm were obtained by cutting the cauda epididymis of a WT or KO mature male mouse and then introduced into TYH medium. We obtained the sperm suspension (10 µl) after pre-incubation and examined the ratio of sperm motility and hyperactivation using an examination plate (Sekisui, Tokyo, Japan) under a microscope (Olympus). The evaluation of the hyperactivation of the sperm followed the criteria and method of Marquez *et al*. as shown in their video images [27]. Briefly, we judged that the flagellar asymmetric motility of the sperm was confirmed in hyperactivation induced sperm and this motility was shown as a ratio of the total sperm (%).

We evaluated the sperm's thermotaxis by examining the sperm's migration ability in a temperature gradient. We controlled the temperature gradient with a stage warmer (MP-10DM., Kitazato, Shizuoka, Japan). After the temperature of the stage warmer was stable, we measured the temperature of the warmer every 10 mm with a radiation thermometer (IR-TAP, Chino, Tokyo, Japan), and we kept the temperature distribution under room temperature.

We prepared a T-shaped chamber (Fig. 1) for the thermotaxis

Table 1. Sets of primers used to amplify mouse TRPV4 homologs from testicular cells

Gene	Forward primer 5'-3'	Reverse primer 5'-3'
Trpv4	CCTTCAGAGACATCTACTACCG	GGATGATAAGTCGGTGACCTC
β-actin	GCTACAGCTTCACCACCACA	CAGGTGGAAGGTCGTCTACA

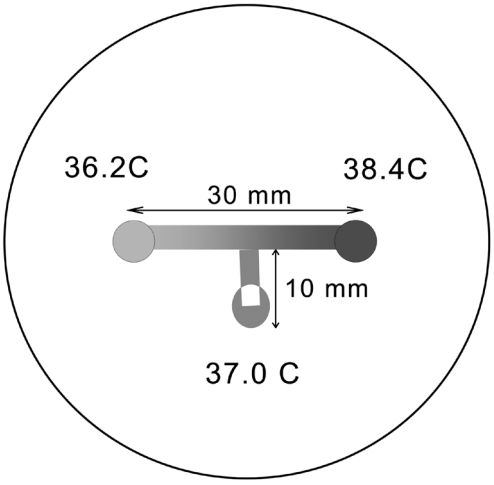

Fig. 1. Diagrammatic demonstration of the T-shaped chamber used for the thermotaxis evaluation of mouse sperm. The chamber consisted of a 10-mm-wide vertical column and a 30-mm-wide horizontal column. The chamber was filled with 15 µl of TYH medium and covered with mineral oil in a 60-mm plastic dish. The temperature gradient of the chamber provided suitable temperature levels for the stage warmer's temperature distribution and was placed on the stage warmer. The sperm was introduced at the end of the vertical column of the chamber. In the temperature gradient condition, the temperature at the low-temperature end of the wide column was 36.2ºC, that at the high-temperature end was 38.4ºC, and the sperm were introduced at the 37.0ºC end of the vertical column and observed for 10 min.

evaluation with a 10-mm-wide vertical column and a 30-mm-wide horizontal column. T-shaped chamber is filled with15 µl of TYH medium and covered with mineral oil in a 60-mm plastic dish (Iwaki, Tokyo, Japan). The temperature gradient of the T-shaped chamber provided suitable temperature levels for the stage warmer's temperature distribution and for the temperature of the 60-mm plastic dish that we placed on the stage warmer. We measured the temperature of the part of the stage warmer equivalent enough to the T-shape chamber after stable temperatures were achieved similarly and confirmed it. All temperature examinations were repeated more than three times. The concentration of the pre-incubated sperm was adjusted to 2×10^4 sperm/ml, and we introduced the sperm at the end of the vertical column of the T-shaped chamber.

In the no-temperature-gradient condition, we set the three ends of the vertical column and wide column to 37.0–37.2ºC, respectively. In the temperature gradient condition, the low-temperature end of the wide column was 36.2ºC, the high temperature was 38.4ºC, and sperm were introduced to the 37.0ºC end of the vertical column and observed for 10 min. We evaluated the sperm's thermotaxis by measuring the numbers of sperm that arrived at the ends of both wide columns after we immobilized the sperm with warming to 60ºC.

The WT sperm that were washed and stained with Hoechst 33342 (9 µM) were mixed with an equal amount of unstained WT sperm, and then migration was examined in the temperature gradient by a method similar to the above description. The migration of Hoechst 33342-stained WT sperm mixed with equal amount of unstained KO sperm were examined in the temperature gradient. We evaluated sperm thermotaxis by examining sperm migration with a microscope (BX40, Olympus) equipped with a fluorescence device (BX-FLA, Olympus).

In the methods mentioned above, 10 µM of Ruthenium red, the TRPV antagonist, was added to a washed sperm suspension and the sperm migration and motility in the temperature gradient were examined.

Statistical analysis

Each experiment was replicated at least four times using sperm from different males. The significance of the differences in sperm motility and migrated sperm numbers were determined with Student's *t*-test and the Mann-Whitney U-test.

Results

Gene expression analysis of the testes cells

The electrophoretic pattern of the PCR products was amplified from the cDNA of WT and KO mouse testes cells. The PCR products amplified by β-actin and a *Trpv4*-specific primer had the molecular weights of 477 bp and 797 bp, respectively. The expression of *Trpv4* gene in the WT mouse testes cells was confirmed. In the KO mouse testes cells, the deletion of the *Trpv4* gene was confirmed (Fig. 2).

Spermatogenesis and sperm morphology

We examined the differentiation and normality of the seminiferous tubule in a *Trpv4* KO mouse after the Periodic Acid Schiff (PAS) staining. We were able to divide spermatogenic waves into 12 stages and the germ cell located in the seminiferous tubule did not show any abnormality in the *Trpv4* KO mouse (Fig. 3).

We examined sperm morphology and acrosomal normality after Coomassie staining. The ratio of abnormal sperm in WT and KO mice is shown in Table 2. The ratio of enlarged head, lost acrosomal, curved-tail and lost-tail sperm were not significantly different between WT and KO mouse sperm (Table 2).

Localization of TRPV4 in mouse sperm

Fluorescence was confirmed in whole sperms, indicating the localization of the TRPV4. In particular, fluorescence intensity in the tail tended to be higher compared to the head (Fig. 4A). The fluorescence intensity of the *Trpv4* KO mouse sperm was lower

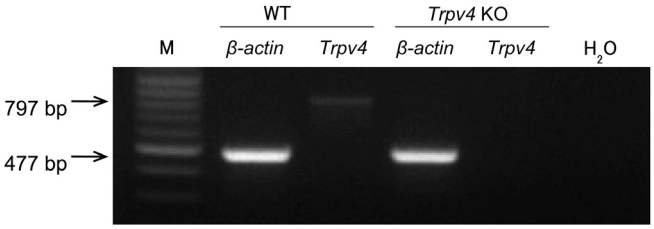

Fig. 2. Reverse transcription PCR products and relative expression of testicular mRNA of *Trpv4* with reference to β-actin mRNA (housekeeping gene) in WT and *Trpv4* KO mouse testes. The RT-PCR products were separated by 2% agarose gel electrophoresis with 100 ng/ml ethidium bromide. M; Marker, WT, *Trpv4* deficient mouse, Negative control in which reverse transcriptase was omitted. In the KO mouse testes cells, the deletion of the *Trpv4* gene was confirmed.

Table 2. Sperm morphology of WT and *Trpv4* KO mice

	Abnormality	WT (%)		KO (%)	
		Mean	± S.E.M.	Mean	± S.E.M.
Head	enlarged	4.9	0.2	5.2	0.3
	acrosome lost	3.3	0.5	3.5	0.4
Tail	curve	6.9	1.8	7.3	1.9
	lost	1.1	0.1	1.2	0.3

than of the WT mouse sperm (Fig. 4B).

Evaluation of sperm motility

The ratio of motility and the ratio of hyperactivation-induced sperm of the WT and *Trpv4* KO mice for the incubation periods up to 4 h are shown in Table 3. The ratio of motile sperm did not show a significant difference between the WT and KO sperm. Over the 4-h incubation, the hyperactivation induction ratio of the sperm increased, but the ratio of the KO mouse sperm was lower than that

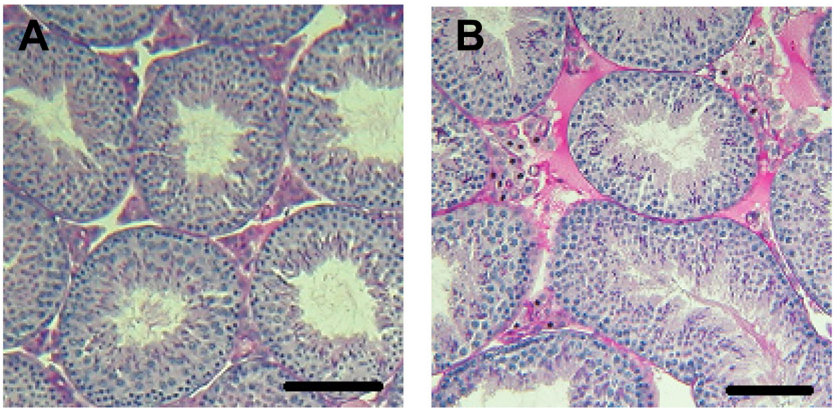

Fig. 3. The PAS-stained tissue samples of a *Trpv4* KO mouse and WT mouse were assessed for normality based on the morphology of the seminiferous tubule. In testes from a KO mouse (B), no histological abnormality was detected in comparison with testes of WT mouse (A). Scale bar, 100 µm.

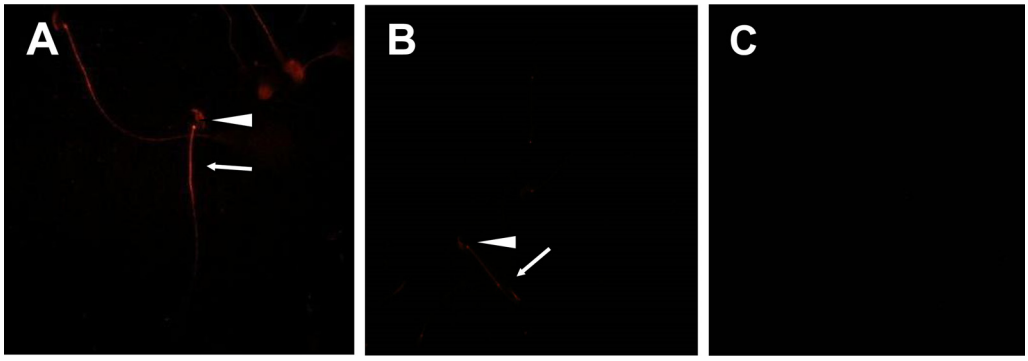

Fig. 4. Immunocytochemical localization of TRPV4 in mature WT (A) and *Trpv4* KO mouse sperm (B). Semen were stained with rabbit anti-mouse TRPV4 antibody. The fluorescence was confirmed in whole sperms, indicating the localization of the TRPV4. In particular, fluorescence intensity tended to be higher in the tail compared to the head (A). The fluorescence intensity of the *Trpv4* KO mouse sperm was lower than that of WT mouse sperm (B). The negative control was reacted with normal rabbit immunoglobulin (C). Arrowhead; sperm head. Arrow; sperm tail.

Table 3. Sperm motility and hyperactivation (HA) of WT and *Trpv4* KO mice

	Inc. (h)	Motility (%)		HA (%)		P-value
		Mean	± S.E.M.	Mean	± S.E.M.	
WT	0	68.3	3.1	1.0	0.3	
	1	68.0	2.8	8.5	1.0	
	2	65.8	2.4	16.0	1.1	
	3	65.0	1.8	30.0	0.0	*
	4	63.3	2.5	28.3	2.0	
KO	0	74.3	0.8	1.5	0.5	
	1	71.3	1.3	1.5	0.5	
	2	70.0	0.0	9.8	1.7	
	3	66.3	2.4	16.5	0.5	*
	4	64.5	1.7	33.9	3.1	

Inc.: Incubation period. * $P < 0.05$ between the WT and KO mouse sperm hyperactivation ratios of the same incubation periods.

of the WT sperm for each incubation period. After the 3-h incubation, the hyperactivation-induced ratios of the WT and KO mouse sperm were 30.0% and 16.5%, respectively, which is significantly lower for the KO mice ($P < 0.05$; Table 3).

Thermotaxis evaluation of the WT mouse sperm

Table 4 shows the numbers of WT mouse sperm that migrated in the T-shaped chamber without a temperature gradient (37.0–37.2ºC), and the numbers of WT mouse sperm observed with the temperature gradient of 36.2–38.4ºC in the chamber's wide column are given in Table 4. In the chamber without the temperature gradient, the WT mouse sperm migrated to the right and left end of the wide column. The averaged ratios of the sperm that migrated to the bilateral ends for all incubation times were 47.4% and 52.6% (Table 4). In the T-shaped chamber with the temperature gradient, the sperm migrated at a high rate in response to high temperatures for all incubation times. The ratio of sperm that migrated in response to a high temperature for all incubation times was significantly higher than that in response to a low temperature ($P < 0.01$). The difference in the ratio of the sperm that migrated to the bilateral ends at 2 h of incubation was remarkable at 30.8%. The average ratios of sperm that migrated to the ends of the chamber in response to the high and low temperatures for all incubation times were 61.7% and 38.3%, respectively (Table 5).

Table 4. WT mouse sperm migration in the column without a temperature gradient (37.0–37.2ºC)

Inc. (h)	Left			Right		
	Mean	± S.E.M.	%	Mean	± S.E.M.	%
0	500.4	51.8	46.8	565.0	56.9	53.2
1	332.6	84.8	49.5	312.4	67.1	50.5
2	306.0	49.4	45.9	360.7	60.7	54.1
3	298.7	53.6	46.8	336.0	61.6	53.2
4	231.0	37.6	47.9	247.2	30.2	52.1

Inc.: Incubation period.

Thermotaxis evaluation of the Trpv4-deficient (KO) mouse sperm

Tables 6 and 7 show the numbers of *Trpv4* gene-deficient (KO) mouse sperm that migrated to the ends of the T-shaped chamber without the temperature gradient (37.2ºC) and in the wide column of the chamber with the temperature gradient of 36.2–38.4ºC, respectively. In the chamber without the temperature gradient, the ratios of sperm that migrated to the bilateral ends before incubation were 47.6% and 52.4%. For all incubation times, the average ratios of the sperm that migrated to the bilateral ends were 48.5% and 51.5% (Table 6).

The KO mouse sperm migrated in response to both the high and low temperatures with the temperature gradient for all incubation times. At all incubation times, the number of sperm that migrated in response to a high temperature was greater than the number that migrated in response to a low temperature (Table 7). The difference in the ratio of the migrated sperm between the ends at the high and low temperature levels for each incubation time ranged from 5% to 9%. The average ratios of sperm that migrated to the chamber ends at the high and low temperatures for all incubation times were 53.8% and 46.2%, respectively (Table 7).

Thermotaxis evaluation of labelled WT mouse sperm

Table 8 shows the number of both WT mouse sperm and Hoechst 33342-labelled WT mouse (labelled) sperm that migrated to the ends of the T-shaped chamber with temperature gradient. For all incubation times, WT mouse sperm and labelled sperm migrated at a high ratio to the high-temperature area. Differences in migration of labelled and unlabelled sperm were not significant. At all incubation times, there was a significantly high ratio of sperm that migrated to the high temperature ($P < 0.01$).

Table 5. WT mouse sperm migration in the column with a temperature gradient (36.2–38.4ºC)

Inc. (h)	Low (36.2°C)			High (38.4°C)			P-value
	Mean	± S.E.M.	%	Mean	± S.E.M.	%	
0	382.9	56.0	39.8	587.7	101.9	60.2	*
1	394.0	56.0	39.1	618.8	86.7	60.9	*
2	261.4	36.2	34.6	491.3	68.7	65.4	*
3	277.9	46.9	41.1	382.0	55.9	58.9	*
4	262.4	53.7	36.9	424.0	77.9	63.1	*

Inc.: Incubation period. * $P < 0.05$ between the Low and High temperature levels of the same incubation period.

Table 6. *Trpv4* KO mouse sperm migration in the column without a temperature gradient (37.0–37.2ºC)

Inc. (h)	Left			Right		
	Mean	± S.E.M.	%	Mean	± S.E.M.	%
0	492.6	30.9	47.6	541.3	33.5	52.4
1	465.0	47.2	51.0	447.7	44.3	49.0
2	492.0	33.0	48.9	518.8	37.7	51.1
3	495.6	70.1	47.2	535.6	39.1	52.8
4	479.8	52.3	48.0	512.6	44.0	52.0

Inc.: Incubation period.

Table 7. *Trpv4* KO mouse sperm migration in the column with a temperature gradient (36.2–38.4ºC)

Inc. (h)	Low (36.2°C)			High (38.4°C)		
	Mean	± S.E.M.	%	Mean	± S.E.M.	%
0	367.9	15.9	47.5	409.0	23.0	52.5
1	366.4	27.7	45.5	441.8	35.5	54.5
2	349.5	12.7	45.6	416.6	8.7	54.4
3	347.4	28.9	45.7	409.4	24.3	54.3
4	310.1	36.9	47.0	343.3	30.0	53.0

Inc.: Incubation period.

Table 8. Labeled* WT mouse sperm migration in the column with a temperature gradient (36.2–38.4ºC)

Inc. (h)	Labeled	Low (36.2ºC)			High (38.4ºC)			P-value
		Mean	± S.E.M.	%	Mean	± S.E.M.	%	
0	–	375.4	48.7	39.0	587.7	85.6	61.0	*
	+	357.9	51.0	40.1	535.1	86.7	59.9	*
2	–	251.3	39.6	35.1	464.9	77.2	65.9	*
	+	237.9	42.3	37.7	393.5	61.2	62.3	*
4	–	244.8	41.7	38.4	393.0	59.3	61.6	*
	+	249.3	49.7	38.3	401.6	63.4	61.7	*

Inc.: Incubation period. * WT mouse sperm were labeled with 9 uM Hoechst 33342. Labeled and unlabeled sperm were mixed in equal volume and introdudced into the chamber; sperm migration was then examined. * $P < 0.05$ between the Low and High temperature levels of the same incubation period.

Table 9 shows the number of both labelled WT mouse sperm and *Trpv4* KO mouse sperm that migrated to the ends of the T-shaped chamber with the temperature gradient. For all incubation times, there was no significant difference between the total number of WT mouse sperm and KO mouse sperm that migrated to the ends. The number of labelled sperm that migrated in response to a high temperature was significantly higher than the number that migrated to a low temperature ($P < 0.01$). For all incubation times, the number of KO mouse sperm that migrated in response to a high temperature was greater than the number that migrated due to a low temperature, but the difference was not significant.

Effect of TRPV4 antagonist on sperm thermotaxis

The motility of Ruthenium red treated WT mouse sperm tended to be lower than that of WT sperm. After 1 h incubation, the ratio of treated sperm that migrated to the high temperature level in the temperature gradient was significantly higher than that which migrated to the lower temperature level. After 2 to 4 h more of incubation, there was no significant difference in the ratio of sperm that migrated to both temperature levels (Table 10).

Discussion

We observed a high rate of positive thermotaxis based on the migration of WT mouse sperm in response to a high temperature level in the temperature gradient set in a T-shaped chamber. The pre-capacitated mouse sperm seemed to show thermotaxis. Bahat *et al*. [11] confirmed the thermotaxis of capacitated rabbit sperm. It is necessary to further clarify the physiological significance and function of the thermotaxis of pre-capacitated mouse sperm.

TRPV4 was detected in rat testes [21], but had not been confirmed in the mouse until now. Some members of the TRPC subfamilies were identified in boar [22], mouse [23] and human sperm [24]. The direct or indirect involvement of TRPV4 in the physiological function of the testes and sperm has been speculated. However, it is not yet known whether other TRPV channels that function as thermo-sensors are present in the sperm.

Delay of the initiation of and increase in the hyperactivation of *Trpv4* KO mouse sperm may be caused by a deficiency of *Trpv4*, which is one of the calcium channels that influence the influx of the calcium ions, which is an important factors in the incubation of hyperactivation in sperm.

Chung *et al*. reported that when Ca^{2+} channel TRPV4 was opened by thermo-stimulation, Ca^{2+} flowed into the sperm and the intracellular Ca^{2+} concentration increased [16, 17]. It was also reported that the Ca^{2+} regulatory mechanism of Ca^{2+} channels or the Na^{+}/Ca^{2+} exchange system on the sperm membrane raises the Ca^{2+} concentrations in the sperm, and involves the change of motility such as hyperactivation or capacitation [2, 28]. The localization and physiological function of the CatSper channel were reported as the channel which participates in the calcium influx to a sperm [29]. The participation of the CatSper channel in the thermotaxis of mouse sperm has not been confirmed. In addition, the physiological function of the CatSper channel in human sperm is its participation in the acrosome reaction by the stimulation of progesterone, and the effects of the CatSper on thermotaxis have not been reported [30].

Table 9. Labeled* WT and unlabeled *Trpv4* KO mouse sperm migration in the column with a temperature gradient (36.2–38.4ºC)

Inc. (h)	Sperm	Low (36.2ºC)			High (38.4ºC)			P-value
		Mean	± S.E.M.	%	Mean	± S.E.M.	%	
0	L*-WT	365.1	39.2	39.6	556.5	45.7	60.4	*
	KO	377.9	20.9	47.2	423.2	19.6	52.8	
2	L*-WT	245.1	49.3	37.0	416.5	51.4	63.0	*
	KO	324.6	22.6	46.1	379.3	12.9	53.9	
4	L*-WT	221.7	59.3	40.9	319.9	60.8	59.1	*
	KO	288.3	55.3	47.2	322.2	33.3	52.8	

Inc.: Incubation period. * WT mouse sperm were labeled with 9uM Hoechst 33342. Labeled (L) WT and unlabeled KO sperm were mixed in equal volume and introdudced into the chamber; sperm migration was then examined. * $P < 0.05$ between the Low and High temperature levels of the same incubation period.

Table 10. Ruthenium red treated WT mouse sperm migration in the column with a temperature gradient (36.2–38.4ºC)

Inc. (h)	Low (36.2°C)			High (38.4°C)			P-value
	Mean	± S.E.M.	%	Mean	± S.E.M.	%	
0	303.3	54.2	43.3	397.7	47.6	56.7	*
1	308.4	45.5	40.9	446.1	55.7	59.1	*
2	219.1	25.2	44.9	268.9	33.3	55.1	
3	228.3	27.5	45.8	270.1	37.4	54.2	
4	220.8	32.4	47.1	248.2	38.5	52.9	

Inc.: Incubation period. * $P < 0.05$ between the Low and High temperature levels of the same incubation period.

The *Trpv4* KO mouse was reported to suffer a loss of the electrophysiological function of TRPV4 [17, 19]. Our present evaluation of the thermotaxis of *Trpv4*-deficient mouse sperm seems to confirm the involvement of TRPV4 in the motility function of mouse sperm. Because offspring were successfully obtained for the *Trpv4*-deficient male mice by natural mating with WT female mice, it is confirmed that the deficiency of the *Trpv4* gene is not a cause of the male sterility.

In species in which sperm thermotaxis has been confirmed, the thermotaxis is thought to provide a physiological function that is extremely important to the motility, migration and motile change associated with sperm capacitation in the female genital tract.

To prove direct involvement of TRPV4 on thermotaxis, we labelled WT sperm with Hoechst 33342, and evaluated thermotaxis in the competitive condition together with *Trpv4* KO mouse sperm. We first confirmed that labelling with Hoechst 33342 did not affect sperm motility or migration. Because evaluation of the migration of Hoechst 33342-labelled sperm had already been confirmed, we examined the thermotaxis of WT sperm and KO sperm by letting them compete at the same time. Results suggested the involvement of TRPV4 in mouse sperm thermotaxis.

Ruthenium red is known to be an antagonist of TRPV. Here, the ratio of WT sperm treated with Ruthenium red that migrated in the temperature gradient decreased during 2 to 4-h incubation. This decrease was similar to that in the migration of *Trpv4* KO mouse sperm and may be dependent on the sperm motility, based on the metabolic changes that occur with the course of the incubation time and a motile change in the hyperactivation-induced sperm. Ruthenium red partially inhibited the migration of WT mouse sperm as it did in *Trpv4* KO mouse sperm. Ruthenium red is known to inhibit not only TRPV4 but also TRPV1, 2, 3 and other TRP subfamilies. Similarly, thermotaxis is caused not only by TRPV4 but also by other TRPV subfamilies.

In light of the low expression of thermotaxis by the *Trpv4*-deficient mouse sperm in the present study, we speculate that sperm thermotaxis may be regulated not by TRPV4 alone, but rather by the associated effects such as other thermo-sensitive factors, e.g., TRP channels or other channel, and ion influx and efflux control factors. In a classification of the temperature-sensitive ranges from 15 to 50ºC, it was reported that TRPV3, TRPM2, TRPM4 and TRPM5 are stimulated in the temperature range of 30–40ºC, that is approximately similar to that in which TRPV4 is stimulated. We therefore suspect that the regulation of the opening and shutting of the calcium channel along with several channels except TRPV4 in the temperature range of 37–39ºC that we examined in this study is associated with sperm thermotaxis, motility, metabolism and signal transduction. Analyses of channels other than TRPV4 and the further elucidation of sperm thermotaxis require additional investigations. Although the details of the underlying mechanism and the signal transduction are unknown, we suggest that TRPV4 and the regulation of the Ca ion influx are associated with mouse sperm thermotaxis.

Bahat *et al.* proposed that human sperm thermotaxis is regulated by the IP3R Ca^{2+} channel and PLC, and that it is not regulated by

TRP channels [8]. In the present study, positive thermotaxis by mouse sperm was confirmed and the expression of *Trpv4* in mouse testes cells was demonstrated. Our findings indicate that TRPV4 plays an important role in the physiology of the sperm that is associated with sperm thermotaxis and fertilization, as we observed differences from the WT sperm with or without Ruthenium red treatment in the *Trpv4*-deficient mouse sperm's migration ability, motility and hyperactivation in the temperature-gradient environment. The elucidation of the thermotaxis of the sperm of mammals including the mouse may advance when similar analyses are conducted for the temperature operation-related calcium channels other than TRPV4.

The thermotaxis that is the conversion of the migration direction of the sperm to a different temperature area was confirmed to be induced by a calcium ion regulating the flagella of the sperm [31], but the details are unknown, and most of the mechanisms of mouse sperm thermotaxis are not known. In addition to the clarification of the sensors and receptors of thermotaxis, it is necessary to perform detailed analyses of thermotaxis including the mechanisms underlying the sperm's migration after direction-changing at a high temperature.

References

1. **Imae Y.** Molecular mechanism of thermosensing in bacteria. *In*: Eisenbach M, Balaban M (eds.), Sensing and Response in Microorganisms. Amsterdam: Elsevirer, 1985:73–81.
2. **Shiba K, Márián T, Krasznai Z, Baba SA, Morisawa M, Yoshida M.** Na^+/Ca^{2+} exchanger modulates the flagellar wave pattern for the regulation of motility activation and chemotaxis in the ascidian spermatozoa. *Cell Motil Cytoskeleton* 2006; **63**: 623–632. [Medline] [CrossRef]
3. **Fabro G, Rovasio RA, Civalero S, Frenkel A, Caplan SR, Eisenbach M, Giojalas LC.** Chemotaxis of capacitated rabbit spermatozoa to follicular fluid revealed by a novel directionality-based assay. *Biol Reprod* 2002; **67**: 1565–1571. [Medline] [CrossRef]
4. **Nara T, Lee L, Imae Y.** Thermosensing ability of Trg and Tap chemoreceptors in Escherichia coli. *J Bacteriol* 1991; **173**: 1120–1124. [Medline]
5. **David A, Vilensky A, Nathan H.** Temperature changes in the different parts of the rabbit's oviduct. *Int J Gynaecol Obstet* 1972; **10**: 52–56.
6. **Hunter RH, Nichol R.** A preovulatory temperature gradient between the isthmus and ampulla of pig oviducts during the phase of sperm storage. *J Reprod Fertil* 1986; **77**: 599–606. [Medline] [CrossRef]
7. **Bahat A, Tur-Kaspa I, Gakamsky A, Giojalas LC, Breitbart H, Eisenbach M.** Thermotaxis of mammalian sperm cells: a potential navigation mechanism in the female genital tract. *Nat Med* 2003; **9**: 149–150. [Medline] [CrossRef]
8. **Bahat A, Eisenbach M.** Human sperm thermotaxis is mediated by phospholipase C and inositol trisphosphate receptor Ca^{2+} channel. *Biol Reprod* 2010; **82**: 606–616. [Medline] [CrossRef]
9. **Bahat A, Eisenbach M.** Sperm thermotaxis. *Mol Cell Endocrinol* 2006; **252**: 115–119. [Medline] [CrossRef]
10. **Bahat A, Eisenbach M, Tur-Kaspa I.** Periovulatory increase in temperature difference within the rabbit oviduct. *Hum Reprod* 2005; **20**: 2118–2121. [Medline] [CrossRef]
11. **Oren-Benaroya R, Orvieto R, Gakamsky A, Pinchasov M, Eisenbach M.** The sperm chemoattractant secreted from human cumulus cells is progesterone. *Hum Reprod* 2008; **23**: 2339–2345. [Medline] [CrossRef]
12. **Guidobaldi HA, Teves ME, Uñates DR, Anastasía A, Giojalas LC.** Progesterone from the cumulus cells is the sperm chemoattractant secreted by the rabbit oocyte cumulus complex. *PLoS ONE* 2008; **3**: e3040. [Medline] [CrossRef]
13. **Montell C.** The TRP superfamily of cation channels. *Sci STKE* 2005; **2005**: re3. [Medline]
14. **Tominaga M, Caterina MJ.** Thermosensation and pain. *J Neurobiol* 2004; **61**: 3–12. [Medline] [CrossRef]
15. **Peier AM, Reeve AJ, Andersson DA, Moqrich A, Earley TJ, Hergarden AC, Story GM, Colley S, Hogenesch JB, McIntyre P, Bevan S, Patapoutian A.** A heat-sensitive TRP channel expressed in keratinocytes. *Science* 2002; **296**: 2046–2049. [Medline] [CrossRef]
16. **Chung MK, Lee H, Caterina MJ.** Warm temperatures activate TRPV4 in mouse 308 keratinocytes. *J Biol Chem* 2003; **278**: 32037–32046. [Medline] [CrossRef]
17. **Chung MK, Lee H, Mizuno A, Suzuki M, Caterina MJ.** TRPV3 and TRPV4 mediate warmth-evoked currents in primary mouse keratinocytes. *J Biol Chem* 2004; **279**: 21569–21575. [Medline] [CrossRef]
18. **Mizuno A, Matsumoto N, Imai M, Suzuki M.** Impaired osmotic sensation in mice lacking *TRPV4*. *Am J Physiol Cell Physiol* 2003; **285**: C96–C101. [Medline] [CrossRef]
19. **Suzuki M, Mizuno A, Kodaira K, Imai M.** Impaired pressure sensation in mice lacking *TRPV4*. *J Biol Chem* 2003; **278**: 22664–22668. [Medline] [CrossRef]
20. **Lee H, Iida T, Mizuno A, Suzuki M, Caterina MJ.** Altered thermal selection behavior in mice lacking transient receptor potential vanilloid 4. *J Neurosci* 2005; **25**: 1304–1310. [Medline] [CrossRef]
21. **Liedtke W, Choe Y, Martí-Renom MA, Bell AM, Denis CS, Sali A, Hudspeth AJ, Friedman JM, Heller S.** Vanilloid receptor-related osmotically activated channel (VR-OAC), a candidate vertebrate osmoreceptor. *Cell* 2000; **103**: 525–535. [Medline] [CrossRef]
22. **Maccarrone M, Barboni B, Paradisi A, Bernabò N, Gasperi V, Pistilli MG, Fezza F, Lucidi P, Mattioli M.** Characterization of the endocannabinoid system in boar spermatozoa and implications for sperm capacitation and acrosome reaction. *J Cell Sci* 2005; **118**: 4393–4404. [Medline] [CrossRef]
23. **Treviño CL, Serrano CJ, Beltrán C, Felix R, Darszon A.** Identification of mouse trp homologs and lipid rafts from spermatogenic cells and sperm. *FEBS Lett* 2001; **509**: 119–125. [Medline] [CrossRef]
24. **Castellano LE, Treviño CL, Rodríguez D, Serrano CJ, Pacheco J, Tsutsumi V, Felix R, Darszon A.** Transient receptor potential (TRPC) channels in human sperm: expression, cellular localization and involvement in the regulation of flagellar motility. *FEBS Lett* 2003; **541**: 69–74. [Medline] [CrossRef]
25. **De Blas GA, Darszon A, Ocampo AY, Serrano CJ, Castellano LE, Hernández-González EO, Chirinos M, Larrea F, Beltrán C, Treviño CL.** TRPM8, a versatile channel in human sperm. *PLoS ONE* 2009; **4**: e6095. [Medline] [CrossRef]
26. **Toyoda Y, Yokoyama M, Hoshi T.** Studies on the fertilization of mouse eggs *in vitro*: I. *In vitro* fertilization of eggs by fresh epididymal sperm. *Jpn J Anim Reprod* 1971; **16**: 147–151. (in Japanese).
27. **Marquez B, Ignotz G, Suarez SS.** Contributions of extracellular and intracellular Ca^{2+} to regulation of sperm motility: Release of intracellular stores can hyperactivate CatSper1 and CatSper2 null sperm. *Dev Biol* 2007; **303**: 214–221. [Medline] [CrossRef]
28. **Quill TA, Sugden SA, Rossi KL, Doolittle LK, Hammer RE, Garbers DL.** Hyperactivated sperm motility driven by CatSper2 is required for fertilization. *Proc Natl Acad Sci USA* 2003; **100**: 14869–14874. [Medline] [CrossRef]
29. **Qi H, Moran MM, Navarro B, Chong JA, Krapivinsky G, Krapivinsky L, Kirichok Y, Ramsey IS, Quill TA, Clapham DE.** All four CatSper ion channel proteins are required for male fertility and sperm cell hyperactivated motility. *Proc Natl Acad Sci USA* 2007; **104**: 1219–1223. [Medline] [CrossRef]
30. **Lishko PV, Botchkina IL, Kirichok Y.** Progesterone activates the principal Ca^{2+} channel of human sperm. *Nature* 2011; **471**: 387–391. [Medline] [CrossRef]
31. **Lindemann CB, Goltz JS.** Calcium regulation of flagellar curvature and swimming pattern in triton X-100—extracted rat sperm. *Cell Motil Cytoskeleton* 1988; **10**: 420–431. [Medline] [CrossRef]